The Solid-State Structures of Dinitrosyliron Iodide and Dinitrosylcobalt Iodide: The Stereochemical Consequences of Strong Metal-Metal Interactions in Ligand-Bridged Complexes

Lawrence F. Dahl,[1a] **Eldrys Rodulfo de Gil,**[1a,2] **and Robert D. Feltham**[1b]

Contribution from the Department of Chemistry, University of Wisconsin, Madison, Wisconsin 53706, and the University of Arizona, Tucson, Arizona 85721. *Received September 16, 1968*

Abstract: Structural determinations of the diamagnetic dinitrosyl iodide complexes of iron and cobalt have revealed that the electron-pair coupling interaction necessary in the iron dinitrosyl complex in order for each iron atom to obtain a closed-shell electronic configuration is sufficiently strong to completely change the solid-state geometries of these iron and cobalt complexes. The crystal structure of $[Fe(NO)_2I]_2$ is comprised of dimeric molecules each formed by the fusion of two identical tetrahedral-like $Fe(NO)_2I_2$ units along the common iodine–iodine edge such that the two iron and two bridging iodine atoms form a planar rhombus. In the solid state cobalt dinitrosyl iodide consists of infinite parallel chains formed by equally oriented tetrahedral-like $Co(NO)_2I_2$ units sharing the common corners of both iodine atoms. Despite the unusually long Fe–Fe electron-pair bond length of 3.05 Å in $[Fe(NO)_2I]_2$ which is 0.17 Å longer than the Fe–Fe bond lengths recorded to date in any nitrosyl or organometallic complex, the different kind and degree of polymerization in $[Fe(NO)_2I]_2$ and $[Co(NO)_2I]_n$ are attributed to the energy stabilization of the dimeric geometry by the formation of the electron pair Fe–Fe bond. The view of a direct Fe–Fe interaction of considerable strength in both the electronically equivalent and structurally analogous $[Fe(NO)_2I]_2$ and $[Fe(NO)_2SC_2H_5]_2$ dimers is strongly supported by the sharply acute bridging Fe–B–Fe angles of only 73–74° in the planar Fe_2B_2 rhombus of each molecule; this angular invariance with a change in the bridging B atoms from sulfur to iodine signifies that the 0.33 Å enlargement of the Fe–Fe internuclear distance in this case is primarily a size effect of the bridging B atoms (*i.e.*, the effective electronegativities of S and I are similar). The constancy of the iron radii (1.23 *vs.* 1.25 Å) derived from the Fe–S and Fe–I bond lengths by subtraction of the presumed single-bond covalent radii of the bridging atoms emphasizes that metal–metal distances in ligand-bridged complexes do *not* generally provide a valid estimate of either metal radii or metal–metal bond orders. A detailed comparison of the molecular features of these and other representative ligand-bridged molecules containing four-membered M_2B_2 bridged systems with and without metal–metal interactions is made. The influential role of the particular coordination about each metal atom in dictating the kind of angular deformation of the M_2B_2 ring from a metal–metal interaction is illustrated for five-, six-, and seven-coordinated metal atoms. It is shown that ligand-bridged complexes containing a known metal–metal electron pair bond (as demonstrated from their magnetic properties) generally can be distinguished from those without metal–metal interactions by their significantly more acute bridging angles. The structural data point to the stability of a complex with an M_2B_2 bridged system being governed not only by the minimization of all nonbonded repulsions between atoms which depend on the sizes of the atoms but also by interorbital electron-pair interactions which for a more electronegative bridging atom favor a wider bridging angle.

Dinitrosyliron iodide, the first known metal nitrosyl halide complex, was originally prepared by Hieber and Anderson[3] from the reaction of iodine with $Fe(NO)_2(CO)_2$. Later, it was found[4-6] that the direct reaction of nitric oxide with the appropriate anhydrous iron and cobalt dihalides (in the presence of the metal powder) yielded nonpolar, sublimable compounds of stoichiometry $Fe(NO)_2X$ (X = Br, I) and $Co(NO)_2X$ (X = Cl, Br, I).

From freezing point molecular weight determinations,[7-9] dipole moment measurements,[9,10] and infrared spectral studies[11,12] carried out in *nonpolar solvents* on various members of these iron and cobalt dinitrosyl halide complexes, a dimeric halogen-bridged structure was

---

[1] (a) University of Wisconsin; (b) University of Arizona.

[2] This manuscript is based in part on a dissertation submitted by E. Rodulfo de Gil to the Graduate School of the University of Wisconsin in partial fulfilment of the requirements for the Ph.D. degree, Aug 1968.

[3] W. Hieber and J. S. Anderson, *Z. Anorg. Allgem. Chem.*, **211**, 132 (1933).

[4] H. Fischer, Dissertation, Technische Hochschule, München, 1937; cited in ref 3.

[5] W. Hieber and R. Marin, *Z. Anorg. Allgem. Chem.*, **240**, 241 (1939).

[6] (a) W. Hieber and R. Nast, *ibid.*, **244**, 23 (1940); (b) *cf.*, W. Hieber and R. Nast, "FIAT Review of German Science, 1939–1946, Anorganische Chemie," Part II, p 146, and references therein.

[7] Molecular weight determinations in benzene were carried out for $Co(NO)_2Cl$[8,9] and $Co(NO)_2Br$.[9] An attempt to determine the molecular weight of $Co(NO)_2I$ in solution was reported[5] to be unsuccessful because of decomposition and low solubility. No mention of a molecular weight determination was found in the literature for $Fe(NO)_2I$.

[8] K. Kelting, Diplomarbeit, Technische Hochschule, München, 1941; cited in ref 6b.

[9] W. Hieber and W. Beck, *Z. Naturforsch.*, **13b**, 194 (1958); *Z. Anorg. Allgem. Chem.*, **305**, 274 (1960).

[10] After correction for atomic polarization effects, a molecular dipole moment equal to 0 D was obtained for $Co(NO)_2Cl$ and $Co(NO)_2Br$ in benzene solutions.

[11] Infrared spectra of the metal dinitrosyl halides in carbon tetrachloride solution were reported by Jahn[12] to have the following two infrared absorption bands in the terminal nitrosyl stretching region: $Fe(NO)_2I$, 1771 and 1818 cm^{-1}; $Co(NO)_2Cl$, 1792 and 1846 cm^{-1}; $Co(NO)_2Br$, 1795 and 1858 cm^{-1}; $Co(NO)_2I$, 1792 and 1846 cm^{-1}. In ethanol solution two nitrosyl frequencies were observed at 1759 and 1843 cm^{-1} for $Co(NO)_2Br$ and 1759 and 1832 cm^{-1} for $Co(NO_2I)$. The considerable shifts of these infrared bands to longer wavelengths in ethanol were attributed[12] to the polarity of the solution.

[12] A. Jahn, *Z. Anorg. Allgem. Chem.*, **301**, 301 (1959).

suggested[12,13] analogous to that found from an X-ray investigation[14] of $[Fe(CO)_3SC_2H_5]_2$. In this structure each metal atom has a tetrahedral-like arrangement of two nitrosyl and two halogen ligands about it with the two tetrahedra linked to each other along the common halogen–halogen edge by the halogen-bridged atoms. An electron spin-coupling interaction is required in the iron complexes but not in the cobalt analogs in order for each of the metal atoms to obtain a closed-shell electronic configuration in agreement with their observed diamagnetism.[15,16] For these iron dinitrosyl halide dimers a direct iron–iron bond was proposed[13,16] similar in nature to that previously suggested[17] for the electronically equivalent diamagnetic Roussin "red" anion, $[Fe(NO)_2S]_2^{2-}$, and its esters including $[Fe(NO)_2SC_2H_5]_2$ for which the X-ray diffraction study[14] showed a rather long iron–iron bonding distance of 2.72 Å.

Preliminary two-dimensional X-ray diffraction studies of $Co(NO)_2Cl$ and $Co(NO)_2Br$ by Corradini and coworkers[18] showed the monoclinic crystalline form of the chloride complex to consist of discrete $[Co(NO)_2Cl]_2$ molecules but revealed a one-dimensional polymeric structure for the bromide complex.[19] The (solid-state) bromide structure is composed of infinite chains, $[Co(NO)_2Br]_n$, in which equivalently oriented $Co(NO)_2$ fragments are connected to one another by singly bridging, collinear bromine atoms. Each cobalt atom thereby has an identical tetrahedral-like environment of two nitrosyl groups and two bromine atoms about it. From the resemblance of the powder patterns of $Co(NO)_2Br$ and $Co(NO)_2I$, Corradini and coworkers[18] suggested that their crystal structures are isomorphous.

While the X-ray investigation of $Co(NO)_2I$ was in progress in this laboratory, the crystal structure of an orthorhombic modification of $Co(NO)_2Cl$ was reported by Jagner and Vannerberg.[20] Their three-dimensional X-ray determination (which was complicated by a crystal twinning and/or a crystal order–disorder phenomena) revealed a crystal structure composed of *ordered* dimeric $[Co(NO)_2Cl]_2$ molecules together with either statistically distributed dimeric molecules or disordered open $\cdots Cl\text{–}Co(NO)_2\text{–}Cl \cdots$ chains, for which the coordination of the four ligands about each cobalt atom is approximately tetrahedral. The proposed disordered chain structure, which Jagner and Vannerberg[20] regarded as somewhat less likely than a disordered dimeric structure, possesses a different conformation from that previously found[18] for $[Co(NO)_2Br]_n$ in that the singly bridging chlorine atoms are not collinear, thereby resulting in two different orientations of the $Co(NO)_2$ fragments with respect to one another.

The over-all objectives which motivated our X-ray examination of $Fe(NO)_2I$ and $Co(NO)_2I$ were: (1) the desirability for a detailed structural comparison between the presumed analogous structures of $[Fe(NO)_2I]_2$ and $[Fe(NO)_2SC_2H_5]_2$ from which the degree of influence of the size of the bridged atoms on this particular molecular geometry (and especially on the iron–iron distance) could be directly appraised in terms of the nature of the electron-pair coupling of the iron atoms in each dimer; (2) the possibility of further assessment of the effect of the iron–iron interaction on the presumed dimeric configuration of $Fe(NO)_2I$ by comparison of appropriate molecular parameters with those of $Co(NO)_2I$; and (3) the opportunity to determine structural interrelationships among the cobalt dinitrosyl halides and related complexes which hopefully would allow the formulation of general stereochemical principles for these halogen-bridged metal complexes containing tetrahedrally coordinated metal atoms.

Experimental Section

Single-Crystal X-Ray Data. Samples of $Fe(NO)_2I$ and $Co(NO)_2I$ were prepared by a modification[21] of the Hieber–Marin method.[5,6] The compounds were purified and crystals obtained by sublimation under vacuum at 60°.

For the iron compound an approximate cubic-shaped crystal of average length of 0.1 mm was mounted in a thin-walled glass capillary which was subsequently evacuated, filled with nitrogen, and then sealed. Multiple-film equiinclination Weissenberg data for reciprocal levels *hk*0 through *hk*5 and timed-exposure precession data for 0*kl*, 1*kl*, and *h*0*l* were taken and merged by a least-squares method[22] to give a total of 769 reflections on a common scale. The weighted disagreement factor for the least-squares merging was 4.2%.

For the cobalt compound difficulties due to twinned intergrowth, air sensitivity, solubility in grease, and softness of the crystals were encountered in attempts to obtain an appropriate single crystal for gathering intensity data. A black plate-like crystal of approximate dimensions 0.05 mm × 0.10 mm × 0.20 mm finally was found which did not show double reflections on either the oscillation or Weissenberg photographs. This crystal was oriented about the 0.20-mm direction inside a thin-walled glass capillary which was evacuated, filled with nitrogen, and then sealed. Multiple-film equiinclination Weissenberg data for reciprocal levels *hk*0 through *hk*4 were collected from which a total of 351 independent reflections were obtained.

All intensity data were taken with Zr-filtered Mo Kα radiation. The intensities of all reflections for each compound were visually estimated with a series of timed exposures of a selected reflection of the same crystal. Corrections for spot extension[23] and Lorentz–polarization effects were applied to all photographic data. For Mo Kα radiation (λ 0.7107 Å) the linear absorption coefficient (μ) for the iron and cobalt compounds of 90.7 and 93.4 cm^{-1}, respectively, results in the same μR_{max} value of 0.45. Since the variation of absorption correction factors with θ is negligible for this μR_{max} value,[24] absorption corrections were not applied. For each compound lattice constants were determined from *h*0*l* and 0*kl* precession photographs taken on a camera calibrated with a NaCl crystal. The γ angle for the monoclinic iron compound was measured from *hk*0 Weissenberg photographs. No extinction or dispersion corrections were made.[25,26]

---

(13) C. C. Addison and J. Lewis, *Quart. Rev.* (London), **9**, 115 (1955).

(14) J. T. Thomas, J. H. Robertson, and E. G. Cox, *Acta Cryst.*, **11**, 599 (1958).

(15) Magnetic measurements by the Gouy technique were made[16] on samples of $Fe(NO)_2I$ and $Co(NO)_2I$ over a temperature range of 85–295 °K and on samples of $Co(NO)_2Cl$ and $Co(NO)_2Br$ at 295 °K. The resulting magnetic gram susceptibilities led to the conclusion that these compounds are all diamagnetic when chemically pure.

(16) H. Soling and R. W. Asmussen, *Acta Chem. Scand.*, **11**, 1534 (1957).

(17) R. G. V. Ewens, *Nature*, **161**, 530 (1948).

(18) F. Bertinotti, P. Corradini, G. Diana, P. Gamis, and C. Pedone, *Ric. Sci. Rend., A*, **3**, 210 (1963).

(19) Although the limited two-dimensional X-ray determinations of $Co(NO)_2Cl$ and $Co(NO)_2Br$ communicated by the Italian workers[18] established their crystal structures, the lack of detailed structural information except for some unrefined (and imprecise) molecular parameters does not permit a comparison of their stereochemical features with those of other compounds.

(20) S. Jagner and N.-G. Vannerberg, *Acta Chem. Scand.*, **21**, 1183 (1967).

(21) B. Haymore and R. D. Feltham, submitted for publication.

(22) P. W. Sutton and M. D. Glick, "A Crystallographic Data Correlation Program for the CDC 1604 Computer," University of Wisconsin, 1964.

(23) D. C. Phillips, *Acta Cryst.*, 7, 746 (1954).

(24) "International Tables for X-Ray Crystallography," Vol. II, The Kynoch Press, Birmingham, England, 1959, p 295.

(25) For Mo Kα radiation the values of the dispersion corrections to the atomic scattering factors are $\Delta f' = 0.4$, $\Delta f'' = 1.0$ for iron; $\Delta f' = 0.4$, $\Delta f'' = 1.1$ for cobalt; $\Delta f' = -0.5$, $\Delta f'' = 2.4$ for io-

Unit Cell and Space Group of $Fe(NO)_2I$ and $Co(NO)_2I$. Deep brown crystals of $[Fe(NO)_2I]_2$ (mol wt, 485.5) are monoclinic with lattice parameters a = 12.30 ± 0.02 Å, b = 12.57 ± 0.02 Å, c = 6.98 ± 0.01 Å, and γ = 109° 58′ ± 25′. The experimental density of 3.19 g/cm^3, determined by flotation in diiodomethane–bromoform solutions, agrees well with the value 3.18 g/cm^3 calculated for four dimers. The observed systematic absences of $\{hk0\}$ with $h + k$ odd and $\{00l\}$ with l odd uniquely define $P2_1/n$ [nonstandard setting of $P2_1/b$ ($C_{2h}{}^5$, no. 14 with c axis unique)] as the probable space group. The subsequent structural analysis showed that the crystallographic asymmetric unit consists of two iron, two iodine, four nitrogen, and four oxygen atoms each occupying the fourfold set of general positions: $\pm(x, y, z;\ {}^1/_2 - x,\ {}^1/_2 - y,\ {}^1/_2 + z)$. These independent atoms comprise two half-molecules such that each of the four dimers in the unit cell possesses a crystallographic center of symmetry.

Crystals of $Co(NO)_2I$ (formula wt, 246) are orthorhombic with lattice parameters a = 10.58 ± 0.03 Å, b = 12.66 ± 0.04 Å, and c = 3.86 ± 0.01 Å. The calculated density of 3.16 g/cm^3 for four $Co(NO)_2I$ species per unit cell is near the experimental value of 3.11 g/cm^3 measured by the flotation method in diiodomethane–bromoform solutions. The observed systematic absences of $\{0kl\}$ with $k + l$ odd and $\{h0l\}$ with h odd indicate the probable space group to be either $Pna2_1$ ($C_{2v}{}^9$, no. 33) or Pnam [nonstandard setting of Pnma ($D_{2h}{}^{16}$, no. 62)]. The observed peak distribution in the three-dimensional Patterson map supported the choice of the centrosymmetric Pnam which was substantiated by the successful refinement of the structure. The structural determination required the location of one cobalt, one iodine, two nitrogen, and two oxygen atoms corresponding to one $Co(NO)_2I$ species as the crystallographic asymmetric unit. All independent atoms were each found to occupy the following set of fourfold special positions (4c) on mirror planes: $\pm(x, y, {}^1/_4;\ {}^1/_2 - x,\ {}^1/_2 + y,\ {}^3/_4)$.

These orthorhombic crystal data for $Co(NO)_2I$ show that this orthorhombic crystalline form is not isomorphous with the observed crystalline form of $Co(NO)_2Br$ which was reported by Corradini and coworkers[18] to be monoclinic with cell dimensions $a \sin \beta$ = 12.45 ± 0.10 Å, b = 10.52 ± 0.10 Å, c = 3.97 ± 0.05 Å, β = 97 ± 3°, and space group $P2_1/a$ ($C_{2h}{}^5$, no. 14 with b axis unique). Nevertheless, by an appropriate transformation of the orthorhombic coordinate system of $Co(NO)_2I$, the crystallographic similarities in the cell dimensions of the bromide and iodide complexes can be readily seen. For $Co(NO)_2I$ the axial transformation $a' = b$, $b' = -a$, $c' = c$ causes Pnam to become equivalent to Pbnm and results in a' = 12.66 Å, b' = 10.58 Å, c' = 3.86 Å. Furthermore, the determined similarity of the *gross* geometries of $Co(NO)_2I$ and $Co(NO)_2Br$ no doubt accounts for the resemblance of their powder patterns.[18,19]

Determination of the Structure. (a) Analysis of $[Fe(NO)_2I]_2$. The crystal structure was elucidated from Patterson and Fourier methods and refined by mixed anisotropic–isotropic least squares to discrepancy factors of $R_1 = [\Sigma||F_o| - |F_c||/\Sigma|F_o|] \times 100$ = 9.6% and $R_2 = [\Sigma w||F_o| - |F_c||^2/\Sigma w|F_o|^2]^{1/2} \times 100$ = 10.5%. A three-dimensional Fourier difference map showed no residual density greater than +1.2 e/Å^3 or less than −1.9 e/Å^3 except in the vicinity of the iodine atoms.

(b) Analysis of $Co(NO)_2I$. All atoms were located from a combination of Patterson and Fourier syntheses. Mixed anisotropic–isotropic least-squares refinement yielded R_1 = 10.3% and R_2 = 11.7%. For this full-matrix refinement, the location of the iodine and cobalt atoms on mirror planes in special positions (4c) of Pnam requires the anisotropic thermal coefficients B_{13} and B_{23} to be zero by symmetry; the B_{33} coefficients for both the iodine and cobalt atoms (calculated from the isotropic thermal parameters obtained from a previous isotropic refinement) were held constant, while the five scale factors (one for each Weissenberg reciprocal level) were allowed to vary. A Fourier difference synthesis based on the output parameters of this refinement revealed no residual density greater than +1.8 e/Å^3 or less than −1.6 e/Å^3 except in the vicinity of the iodine atoms.

Table I. Final Atomic Parameters of $[Fe(NO)_2I]_2$ with Standard Deviations

Atom	x	y	z	B
I(1)	−0.0609 (2)	0.0594 (2)	0.2411 (2)	a
Fe(1)	0.0604 (3)	0.1201 (3)	−0.0646 (6)	a
N(1–1)	−0.0087 (23)	0.1846 (23)	−0.2161 (35)	3.7 (5)
N(2–1)	0.1970 (22)	0.1914 (21)	−0.0065 (38)	4.0 (5)
O(1–1)	−0.0257 (24)	0.2526 (26)	−0.2831 (37)	6.0 (6)
O(2–1)	0.2848 (24)	0.2609 (22)	0.0260 (43)	7.1 (7)
I(2)	0.0637 (2)	0.4397 (2)	0.2649 (2)	a
Fe(2)	−0.1246 (3)	0.4441 (3)	0.4245 (6)	a
N(1–2)	−0.1857 (21)	0.5094 (23)	0.2794 (32)	3.4 (5)
N(2–2)	−0.2055 (26)	0.3145 (26)	0.4831 (47)	5.7 (7)
O(1–2)	−0.2519 (23)	0.5290 (20)	0.1688 (38)	5.2 (5)
O(2–2)	−0.2801 (24)	0.2266 (23)	0.4815 (43)	7.3 (7)

[a] Anisotropic temperature factors of the form $\exp\{-[B_{11}h^2 + B_{22}k^2 + B_{33}l^2 + 2B_{12}hk + 2B_{13}hl + 2B_{23}kl]\}$ were utilized for the iodine and iron atoms; the resulting thermal coefficients (× 10^4) with esd of last significant figures given in parentheses are

Atom	B_{11}	B_{22}	B_{33}	B_{12}	B_{13}	B_{23}
I(1)	82 (2)	82 (2)	217 (5)	23 (1)	16 (2)	10 (2)
I(2)	73 (2)	84 (2)	228 (6)	27 (1)	0 (2)	−21 (2)
Fe(1)	42 (3)	48 (3)	220 (11)	6 (2)	−11 (5)	19 (5)
Fe(2)	50 (3)	51 (3)	210 (10)	12 (2)	−14 (5)	15 (5)

Table II. Final Atomic Parameters of $[Co(NO)_2I]_n$ with Standard Deviations

Atom	x	y	z	B
I	0.5887 (2)	0.3487 (2)	0.25	a
Co	0.4411 (3)	0.2892 (4)	0.75	a
N(1)	0.3152 (34)	0.3613 (26)	0.75	5.4 (6)
N(2)	0.4247 (35)	0.1634 (34)	0.75	6.8 (9)
O(1)	0.2137 (45)	0.3955 (35)	0.75	10.8 (11)
O(2)	0.3989 (38)	0.0721 (43)	0.75	10.7 (12)

[a] For the I and Co atoms anisotropic temperature factors of the form $\exp\{-[B_{11}h^2 + B_{22}k^2 + B_{33}l^2 + 2B_{12}hk + 2B_{13}hl + 2B_{23}kl]\}$ were used; the resulting thermal coefficients with standard deviations of the last significant figures given in parentheses are

Atom	B_{11}	B_{22}	B_{33}	B_{12}	B_{13}	B_{23}
Co	63 (4)	82 (3)	654	−6 (3)	0	0
I	88 (2)	110 (2)	774	−16 (1)	0	0

All least-squares refinements were calculated with a local version of the Busing–Martin–Levy OR FLS program.[27] The function minimized was $\Sigma w||F_o|_o - |F_c||^2$ where individual weights were assigned to the observed structure factors according to the function $\sqrt{w} = 20/F_o$ if $I_o \geqslant 4I_o(\text{min})$ and $\sqrt{w} = 1.25I_o{}^2/F_oI_o{}^2(\text{min})$ if $I_o < 4I_o(\text{min})$. The scattering factors utilized in these structural analyses were those of Thomas and Umeda[28] for iodine, iron, and cobalt and those of Berghuis, *et al.*,[29] for nitrogen and oxygen.

All Patterson and Fourier summations were computed with the Blount program.[30] The positional and thermal parameters of $[Fe(NO)_2I]_2$ and $Co(NO)_2I$ obtained from the output of the last

---

dine.[26] Since both the iron and cobalt dinitrosyl iodide crystals possess centrosymmetric space groups, these relatively small dispersion corrections are presumed not to affect significantly the atomic coordinates in either compound.[26]

(26) D. H. Templeton in "International Tables for X-Ray Crystallography," Vol. III, The Kynoch Press, Birmingham, England, 1962, p 215; D. H. Templeton, *Acta Cryst.*, **8**, 842 (1955).

(27) W. R. Busing, K. O. Martin, and H. A. Levy, "OR FLS, A Fortran Crystallographic Least-Squares Program," ORNL-TM-305, Oak Ridge National Laboratory, 1963.

(28) L. H. Thomas and K. Umeda, *J. Chem. Phys.*, **26**, 293 (1957).

(29) J. Berghuis, IJ. M. Haanappel, M. Potters, B. O. Loopstra, C. H. MacGillavry, and A. L. Veenendaal, *Acta Cryst.*, **8**, 478 (1955).

(30) J. F. Blount, "A Three-Dimensional Crystallographic Fourier Summation Program for the CDC 1604 Computer," Ph.D. Thesis (Appendix), University of Wisconsin, 1965.

Table III. Distances and Angles of $[Fe(NO)_2I]_2$ with Their Standard Deviations

	A. Intramolecular Distances (Å)		
Fe(1)–Fe(1′)	3.013 (7)	Fe(1)···O(1–1)	2.72 (2)
Fe(2)–Fe(2′)	3.089 (7)	Fe(1)···O(2–1)	2.79 (2)
		Fe(2)···O(1–2)	2.81 (2)
	3.05 (av)	Fe(2)···O(2–2)	2.78 (2)
I(1)···I(1′)	4.165 (4)		2.78 (av)
I(2)···I(2′)	4.140 (4)		
		N(1–1)···N(2–1)	2.90 (3)
	4.15 (av)	N(1–2)···N(2–1)	2.77 (3)
Fe(1)–I(1)	2.567 (4)		2.84 (av)
Fe(1)–I(1′)	2.573 (5)		
Fe(2)–I(2)	2.589 (4)	I(1)···N(1–1)	3.52 (2)
Fe(2)–I(2′)	2.576 (5)	I(1′)···N(1–1)	3.46 (2)
		I(1)···N(2–1)	3.49 (2)
	2.58 (av)	I(1′)···N(2–1)	3.43 (2)
		I(2)···N(1–2)	3.47 (2)
Fe(1)–N(1–1)	1.73 (3)	I(2′)···N(1–2)	3.48 (2)
Fe(1)–N(2–1)	1.66 (2)	I(2)···N(2–2)	3.49 (3)
Fe(2)–N(1–2)	1.64 (2)	I(2′)···N(2–2)	3.46 (2)
Fe(2)–N(2–2)	1.65 (3)		
			3.48 (av)
	1.67 (av)		
N(1–1)–O(1–1)	1.06 (3)		
N(2–1)–O(2–1)	1.16 (3)		
N(1–2)–O(1–2)	1.21 (3)		
N(2–2)–O(2–2)	1.17 (4)		
	1.15 (av)		
	B. Bond Angles (Degrees)		
I(1)–Fe(1)–I(1′)	108.2 (1)	I(1)–Fe(1)–N(1–1)	108.5 (8)
I(2)–Fe(2)–I(2′)	106.6 (1)	I(1)–Fe(1)–N(2–1)	109.6 (9)
		I(1′)–Fe(1)–N(1–1)	105.5 (8)
	107.4 (av)	I(2)–Fe(2)–N(2–1)	106.5 (8)
		I(2)–Fe(2)–N(1–2)	108.2 (8)
Fe(1)–I(1)–Fe(1′)	71.8 (1)	I(2)–Fe(2)–N(2–2)	109.2 (10)
Fe(2)–I(2)–Fe(2′)	73.4 (1)	I(2′)–Fe(2)–N(1–2)	109.3 (8)
		I(2′)–Fe(2)–N(2–2)	108.1 (10)
	72.6 (av)		
			108 (av)
N(1–1)–Fe(1)–N(2–1)	117.8 (12)		
N(1–2)–Fe(2)–N(2–2)	115.0 (13)	Fe(1)–N(1–1)–O(1–1)	157 (3)
		Fe(1)–N(2–1)–O(2–1)	165 (3)
	116 (av)	Fe(2)–N(1–2)–O(1–2)	163 (2)
		Fe(2)–N(2–2)–O(2–2)	161 (3)
O(1–1)···Fe(1)···O(2–1)	99 (3)		
O(1–2)···Fe(2)···O(2–2)	97 (3)		161 (av)
	98 (av)		
	C. Closest Intermolecular Distances (Å)		
O(1–1)···N(2–2)[b]	3.05 (3)	O(2–1)···O(1–1)[a]	3.30 (3)
O(2–1)···N(1–1)[a]	3.16 (3)	O(1–1)···O(2–2)[b]	3.44 (3)
O(2–1)···N(2–1)[a]	3.31 (4)	O(2–1)···O(2–1)[a]	3.58 (1)
O(1–1)···I(2)[b]	3.86 (2)	O(2–1)···Fe(1)[a]	3.47 (2)
I(1)···O(2–1)[a]	3.91 (2)	O(1–1)···Fe(2)[b]	3.66 (2)

[a] For position $0.5 - x, 0.5 - y, 0.5 + z$. [b] For position $b = x, y, z - 1.0$.

least-squares cycle are presented in Tables I and II.[31] Tables III and IV give the distances and bond angles with estimated standard deviations, calculated with the Busing–Martin–Levy function and error program[32] from the full inverse matrix (containing estimated lattice parameter errors).

Mass Spectral Data. The mass spectra of both $Fe(NO)_2I$ and $Co(NO)_2I$ were obtained from the Hitachi Perkin–Elmer double-focusing mass spectrometer Model RMV-6E located at the University of Arizona. The operating conditions were 70-eV electron energy and 60° inlet temperature with samples introduced through the liquid inlet. The relative peak intensities were obtained from the peak heights. Table V records the *m/e* of the major peaks along with their relative abundances for the unreported $Fe(NO)_2I$ dimer.

Results and Discussion

Description of the Structures. The crystal structure of $[Fe(NO)_2I]_2$ is comprised of dimeric molecules which ideally possess D_{2h}-2/m2/m2/m symmetry; the required

---

[31] Calculated and observed structure factors for $[Fe(NO)_2I]_2$ and $[Co(NO)_2I]_n$ are deposited as Document No. NAPS-00192 with the ASIS National Auxiliary Publication Service, c/o CCM Information Science, Inc., 22 West 34th St., New York, N. Y. 10001. A copy may be secured by citing the document number and remitting $1.00 for microfiche or $3.00 for 35 photocopies. Advance payment is required. Make checks or money orders payable to: ASIS-NAPS.

[32] W. R. Busing, K. O. Martin, and H. A. Levy, "OR FFE, A Fortran Crystallographic Function and Error Program," ORNL-TM-306, Oak Ridge National Laboratory, 1964.

Table IV. Distances and Angles of $[Co(NO)_2I]_n$ with Their Standard Deviations

	A. Intrachain Distances (Å)		
Co···Co	3.864 (3)	Co···O(1)	2.76 (5)
		Co···O(2)	2.78 (5)
I···I	3.864 (3)		
			2.77 (av)
Co–I	2.593 (3)		
		N(1)···N(2)	2.75 (5)
Co–N(1)	1.61 (4)		
Co–N(2)	1.60 (4)	I···N(1)	3.48 (3)
		I···N(2)	3.49 (3)
	1.61 (av)		
			3.49 (av)
N(1)–O(1)	1.16 (5)		
N(2)–O(2)	1.19 (5)		
	1.17 (av)		
	B. Bond Angles (Degrees)		
I–Co–I	96.2 (1)	N(1)–Co–I	109.3 (8)
		N(2)–Co–I	110.7 (8)
Co–I–Co	96.2 (1)		
			110 (av)
N(1)–Co–N(2)	118.3 (18)		
		Co–N(1)–O(1)	168 (4)
O(1)···Co···O(2)	110.0 (13)	Co–N(2)–O(2)	173 (4)
			171 (av)
	C. Closest Interchain Distances (Å)		
N(2)–O(1)[b]	3.14 (6)	I–O(1)[a]	3.85 (4)
O(1)–O(2)[c]	3.18 (5)	O(1)–I[a]	3.85 (4)
O(2)–O(1)[b]	3.35 (5)	I–O(1)[b]	3.87 (3)
N(1)–I[a]	3.80 (3)	I–O(2)[b]	3.93 (3)
I–N(1)[a]	3.80 (3)	Co–O(1)[b]	3.71 (4)

[a] For position $1 - x, 1 - y, 1 - z$. [b] For position $0.5 + x, 0.5 - y, z$. [c] For position $0.5 - x, 0.5 + y, 0.5 + z$.

Table V. Mass Spectrum of $[Fe(NO)_2I]_2$

Species	m/e	Rel abundance
$Fe_2(NO)_4I_2^+$	486	10
$Fe_2(NO)_3I_2^+$	456	25
$Fe_2(NO)_2I_2^+$	426	15
$Fe_2(NO)I_2^+$	396	10
$Fe_2I_2^+$	366	24
I_2^+	254	17
Fe_2I^+	239	5
FeI^+	183	10
I^+	127	15
Fe_2^+	112	2
$Fe(NO)^+$	86	1
Fe^+	56	5

crystallographic molecular symmetry is C_i-$\bar{1}$. Each iron atom is coordinated to two nitrosyl groups and to two iodine atoms at the corners of a somewhat distorted tetrahedron. The dimeric configuration, given with mean bond lengths and angles in Figure 1, formally arises from a fusion of the two identical tetrahedral units along the common iodine–iodine edge such that the two iron and two bridging iodine atoms form a planar rhombus. The packing of the four dimeric molecules in the unit cell is shown in Figure 2. The closest intermolecular approaches of 3.3 Å for O···O contacts, 3.6 Å for N···O contacts, and 3.9 Å for I···O contacts are all greater than van der Waals distances and hence support the premise that there are no unusual intermolecular interactions.

In the solid state $Co(NO)_2I$ consists of infinite chains parallel to the c axis formed by equally oriented $Co(NO)_2I_2$ tetrahedra sharing the corners of both iodine atoms.

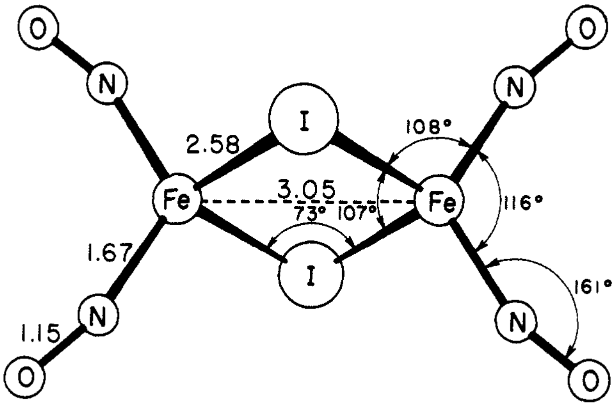

Figure 1. The molecular configuration of $[Fe(NO)_2I]_2$.

Figure 3 shows a section of the $[Co(NO)_2I]_n$ chain for which the ···I–$Co(NO)_2$–I··· part corresponds to one unit cell in periodicity of length c = 3.86 Å. The localized intrachain site symmetry at each cobalt atom (and also at each iodine atom) ideally is C_{2v}-2mm; the crystallographically demanded symmetry at each atom is C_s-m with the independent iodine atom located on the mirror plane at $z = {}^1/_4$ and the independent $Co(NO)_2$ fragment oriented on the mirror plane at $z = {}^3/_4$. Figure 4 displays the packing of the four parallel chains in the unit cell. The minimum distances between chains are 3.1 Å for O···N contacts, 3.2 Å for O···O contacts, 3.8 Å for I···N contacts, and 3.85 Å for I···O contacts; these large interchain distances which are all greater than van der Waals distances indicate the absence of any

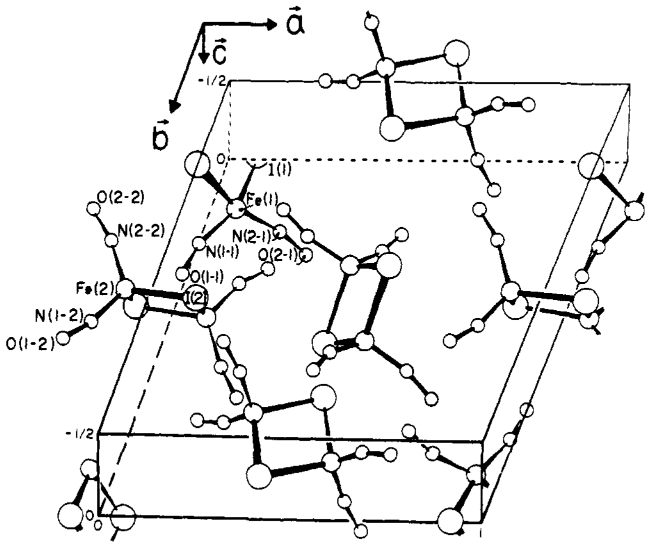

Figure 2. Arrangement of the $[Fe(NO)_2I]_2$ molecules as viewed in one-half the unit cell of volume $a \times b \times {}^1/_2c$.

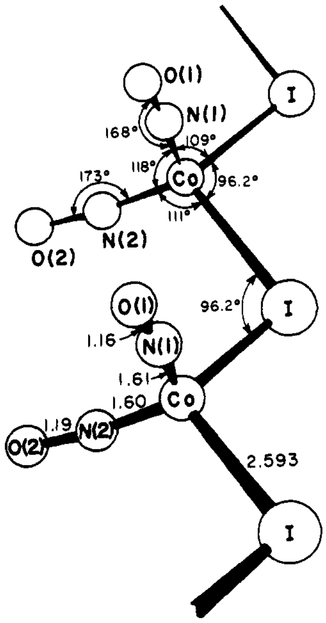

Figure 3. A section of the infinite chain of $[Co(NO)_2I]_n$.

abnormal interchain interactions which would significantly influence the intrachain geometry.

Structural and Bonding Relationships between $[Fe(NO)_2I]_2$ and $[Fe(NO)_2SC_2H_5]_2$. (a) The Heterocyclic Fe_2B_2-Bridged System. An important structural feature which emerges from a detailed comparison of the molecular parameters of the electronically equivalent and structurally analogous $[Fe(NO)_2I]_2$ and $[Fe(NO)_2SC_2H_5]_2$[14] is the maintenance of identical angles in the planar Fe_2B_2 rhombus with a change in the bridging B atoms from sulfur to iodine, *viz.* 74 *vs.* 73° for the Fe–S–Fe and Fe–I–Fe angles, respectively; 106 *vs.* 107° for the S–Fe–S and I–Fe–I angles, respectively. This particular invariance in the angular dimensions of the Fe_2B_2 bridging system indicates that the 0.33 Å enlargement of the Fe–Fe internuclear distance from 2.72 to 3.05 Å is primarily due to the different sizes of the bridging B atoms in increasing the

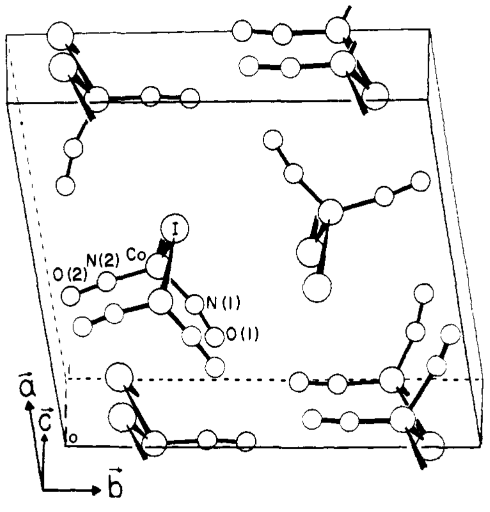

Figure 4. The packing of the four infinite chains of $[Co(NO)_2I]_n$ in the unit cell.

Fe–B distance from 2.27 to 2.58 Å. The interatomic distances and angles in $[Fe(NO)_2SC_2H_5]_2$ are close to the corresponding ones in Roussin's black salt, $CsFe_4S_3(NO)_7 \cdot H_2O$.[33,34]

(b) Nature of the Iron–Iron Bond. The iron–iron bond length of 3.05 Å in $[Fe(NO)_2I]_2$ is 0.17 Å longer than the iron–iron bond lengths previously found in any iron carbonyl, nitrosyl, or cyclopentadienyl complex; the recorded iron–iron electron pair bonds in these complexes[35-44] range from 2.37 Å in $Fe_2(CO)_6(C_6H_5NC_6H_4NH)$[37] to 2.88 Å both in the $Fe_2(CO)_8{}^{2-}$ anion[43] and in $Fe_2(CO)_6[(CH_3)_4As_2C_2C_2F_4]$.[44] In the $[Fe(NO)_2SC_2H_5]_2$ complex[14] the iron–iron bond of 2.72 Å also ranks among the longer known iron–iron values. The constancy of the iron radii (1.23 *vs.* 1.25 Å) derived from the Fe–S and Fe–I bond lengths by subtraction of the presumed single-bond covalent radii of the bridging atoms (see Table VI)[45] thereby reinforces the previously drawn conclusion[36] that in general metal–metal distances in

---

(33) G. Johansson and W. N. Lipscomb, *Acta Cryst.*, **11**, 594 (1958).

(34) The diamagnetic anion, $Fe_4S_3(NO)_7{}^-$, of approximate C_{3v} symmetry can be formally considered to be comprised of three molecules of the red ethyl ester (minus the ethyl groups and five NO groups) which are fused together along two adjacent Fe–S edges. Each of the three resulting equivalent basal $Fe(NO)_2$ fragments, connected to one another by the three triply bridging sulfur atoms (but no Fe–Fe bonds), is bonded to the apical Fe(NO) fragment by two of the triply bridging sulfur atoms and by an Fe–Fe bond. Not only is the localized tetrahedral-like bonding environment of two sulfur and two nitrosyl ligands about each of the three basal iron atoms identical with that about each iron atom in $[Fe(NO)_2SC_2H_5]_2$ but also the mean molecular dimensions of each of the three bonding Fe_2S_2 systems closely parallel those of the Fe_2S_2 rhombus in $[Fe(NO)_2SC_2H_5]_2$ (*viz.* the Fe–S side of 2.23 *vs.* 2.27 Å; the identical Fe–S–Fe and S–Fe–S angles of 74° and 106°, respectively; the Fe–Fe bond distance of 2.70 *vs.* 2.72 Å; and the nonbonding S···S distance of 3.52 *vs.* 3.63 Å).

(35) For an extensive compilation of iron–iron distances, see M. R. Churchill, *Inorg. Chem.*, 6, 190 (1967).

(36) L. F. Dahl, W. R. Costello, and R. B. King, *J. Am. Chem. Soc.*, **90**, 5422 (1968), and references cited therein.

(37) P. E. Baikie and O. S. Mills, *Chem. Commun.*, 707 (1966); *Inorg. Chim. Acta*, **1**, 55 (1967).

(38) R. J. Doedens, *Inorg. Chem.*, **7**, 2323 (1968).

(39) R. E. Davis, Abstracts of Papers, National Meeting of the American Crystallographic Association, Tucson, Ariz., Feb 1968, p 30.

(40) O. S. Mills and A. D. Redhouse, *Chem. Commun.*, 444 (1966).

(41) J. Meunier-Piret, P. Piret, and M. Van Meersche, *Bull. Soc. Chim. Belges*, **76**, 364 (1967).

(42) (a) F. A. Cotton and M. D. LaPrade, *J. Am. Chem. Soc.*, **90**, 2026 (1968); (b) F. A. Cotton and J. Takats, *ibid.*, **90**, 2031 (1968).

(43) O. S. Mills, private communication to L. F. Dahl, 1961; O. S. Mills and F. S. Stephens, submitted for publication.

(44) F. W. B. Einstein and J. Trotter, *J. Chem. Soc.*, *A*, 824 (1967).

Table VI. Comparison of Mean Geometrical Parameters of $[Fe(NO)_2I]_2$ and $[Co(NO)_2I]_n$ with Those of Representative Compounds Containing Four-Membered Heterocyclic Ring M_2B_2 Systems with and without Metal–Metal Interactions[a]

Molecule	No.	Source	Distance, Å M–M	 M–B	 B···B	van der Waal's B···B distance, Å	Distance, Å 1/2(M–M)	Radius, Å {(M–B)–B_{radius}}[b]	Angle, deg M–B–M	 B–M–B	c
					A. Ligand-Bridged Metal Complexes Containing Metal–Metal Interactions						
$[Fe(NO)_2I]_2$ (B = I)	I	This work	3.05	2.58	4.15	4.3	1.52	1.25	73	107	180
$[Fe(NO)_2SC_2H_5]_2$ (B = S)	II	*g*	2.72	2.27	3.63	3.7	1.36	1.23	74	106	180
$[Fe(CO)_3SC_2H_5]_2$ (B = S)	III	*h*	2.54	2.26	2.93	3.7	1.27	1.22	68	81	95
$[Fe(CO)_3NH_2]_2$ (B = N)	IV	*i*	2.40	1.98	2.50	3.0	1.20	1.28	74	78	78
$[Co(\pi\text{-}C_5H_5)P(C_6H_5)_2]_2$ (B = P)	V	*j*	2.56	2.16	2.88	3.8	1.28	1.06	72.5	84	105
α-$[NbI_4]_n$ (B = I)[d]	VI	*k*	3.31	2.74	4.37	4.3	1.65	1.41	74	106	180
					B. Ligand-Bridged Metal Coinplexes Containing No Metal–Metal Interactions						
α-$[NbI_4]_n$ (B = I)[d]	VI	*k*	4.36	2.90	3.81	4.3	. . .	1.57	98	82	180
$[Co(NO)_2I]_n$ (B = I)	VII	This work	3.86	2.59	3.86	4.3	. . .	1.26	96	96	. . .
$[InI_3]_2$ (B = I)	VIII	*l*	3.88	2.84	4.14	4.3	. . .	1.51	86	94	180
$[NbI_5]_2$ (B = I)	IX	*m*	4.55	2.99	3.83	4.3	. . .	1.66	100	80	180
$[Co(NO)_2Cl]_2$ (B = Cl)[e]	X	*n*	3.20	2.13 2.33	3.12	3.6	. . .	1.14 1.34	92	88	180
$[FeCl_3]_2$(v) (B = Cl)[f]	XI	*o*	2.96	2.17	3.17	3.6	. . .	1.18	96	84	180
$[BeCl_2]_n$ (B = Cl)	XII	*p*	2.63	2.02	3.05	3.6	. . .	1.03	82	98	180
$[AlCH_3Cl_2]_2$ (B = Cl)	XIII	*q*	3.21	2.26	3.15	3.6	. . .	1.27	91	89	180
$[GaCl_3]_2$ (B = Cl)	XIV	*r*	3.12	2.29	3.35	3.6	. . .	1.30	86	94	180
$[PdCl_2]_n$ (B = Cl)	XV	*s*	3.35	2.31	3.18	3.6	. . .	1.32	93	87	180
$[NbCl_5]_2$ (B = Cl)	XVI	*t*	3.90	2.53	3.22	3.6	. . .	1.54	101	79	180
$[Ni(\pi\text{-}C_5H_5)P(C_6H_5)_2]_2$ (B = P)	XVII	*j*	3.36	2.15	2.70	3.8	. . .	1.05	102	78	180
$[AlBr_3]_2$ (B = Br)	XVIII	*u*	3.14	2.38	3.59	3.9	. . .	1.24	82	98	180
$[Mg(C_2H_5)N(C_2H_5)_3Br]_2$ (B = Br)	XIX	*v*	3.53	2.57	3.72	3.9	. . .	1.43	87	93	180
$[Mn(CO)_4Br]_2$ (B = Br)	XX	*w*	3.74	2.53	3.39	3.9	. . .	1.39	96	84	180

[a] Where M represents the metal atom and B the metal-linked bridging atom. [b] The following B_{radius} values were used for the bridging atom B corresponding to Pauling's estimated single-bond tetrahedral-like covalent radii: N, 0.70 Å; P, 1.10 Å; S, 1.04 Å; Cl, 0.99 Å; Br, 1.14 Å; I, 1.33 Å. [c] Dihedral angle between the two planes in the M_2B_2 system each formed by the two bridging B atoms and one M atom. This angle is defined as the angle directly between the two planes rather than as the angle between the normals to the planes. [d] The linear chain structure of α-$[NbI_4]_n$ formed by NbI_6 octahedra sharing two opposite edges contains two kinds of Nb_2I_2 ring systems; one with and the other without a Nb–Nb electron-pair interaction, which alternate with each other. [e] The recorded values are the molecular parameters for only the ordered dimer in the unit cell of $[Co(NO)_2Cl]_2$. [f] If the imprecisely known molecular parameters obtained by a nonrecent electron diffraction study of $[FeCl_3]_2$ gas (which condenses in the solid state to a layer-like nonmolecular structure) are assumed to be approximately correct, the reported Fe–Fe distance of only 2.96 Å leads to the speculation that partial spin pairing of the normally five unpaired electrons in each Fe(III) may occur for the vapor-state dimeric molecule. Unlike the sharply acut M–B–M angles of the diamagnetic metal complexes (I–VI) containing electron spin-coupling metal–metal interactions, the reported Fe–Cl–Fe angle of 96° is obtuse. [g] J. T. Thomas, J. H. Robertson, and E. G. Cox, *Acta Cryst.*, **11**, 599 (1958). [h] L. F. Dahl and C. H. Wei, *Inorg. Chem.*, **2**, 328 (1963). [i] L. F. Dahl, W. R. Costello, and R. B. King, *J. Am. Chem. Soc.*, **90**, 5422 (1968). [j] J. M. Coleman and L. F. Dahl, *ibid.*, **89**, 542 (1967). [k] L. F. Dahl and D. L. Wampler, *Acta Cryst.*, **15**, 903 (1962). [l] J. D. Forrester, A. Zalkin, and D. H. Templeton, *Inorg. Chem.*, **3**, 63 (1964). [m] L. F. Dahl and N. Nelson, unpublished research. [n] S. Jagner and N.-G. Vannerberg, *Acta Chem. Scand.*, **21**, 1183 (1967). [o] *Cf.* A. F. Wells, "Structural Inorganic Chemistry," 3rd ed, the Clarendon Press, Oxford, 1962, p 356. [p] R. E. Rundle and P. H. Lewis, *J. Chem. Phys.*, **20**, 132 (1952). [q] G. Allegra, G. Perego, adn A. Immirzi, *Makromol. Chem.*, **61**, 69 (1963). [r] S. C. Wallwork and I. J. Worrall, *J. Chem. Soc.*, 1816 (1965). [s] A. F. Wells, *Z. Krist.*, **100**, 189 (1939). [t] A. Zalkin and D. E. Sands, *Acta Cryst.*, **11**, 615 (1958). [u] P. A. Renes and C. H. MacGillavry, *Rec. Trav. Chim.*, **64**, 275 (1945). [v] J. Toney and G. D. Stucky, *Chem. Commun.*, 1168 (1967). [w] L. F. Dahl and C. H. Wei, *Acta Cryst.*, **16**, 611 (1963).

ligand-bridged complexes do *not* provide a valid estimate of either metal radii or metal–metal bond orders.

In both $[Fe(NO)_2I]_2$ and $[Fe(NO)_2SC_2H_5]_2$ the observed diamagnetism requires either a distinct electron-pair iron–iron bond formed by direct iron orbital overlap or a superexchange phenomenon involving an electron-pair coupling through the bridging ligand groups. It is presumed that this latter antiferromagnetic interaction would *not* appreciably change the M_2B_2 ring geometry of the metal and bridging B atoms from that for which no metal–metal interaction occurs.

From their X-ray analysis of $[Fe(NO)_2SC_2H_5]_2$, Thomas, Robertson, and Cox[14] commented that the Fe–Fe distance of 2.72 Å is much longer than that of 2.46 Å found in $Fe_2(CO)_9$. Since they felt that this latter distance corresponds to a single bond, they implied (by their nonbonding notation of Fe···Fe) that (although the interaction between the iron atoms in $[Fe(NO)_2SC_2H_5]_2$ must be strong enough to account for the observed dia-

(45) In light of Pauling's estimated covalent radii for Fe (1.16 Å), Co (1.16 Å), Ni (1.15 Å), N (0.70 Å), P (1.10 Å), S (1.04 Å), and I (1.33 Å), the close similarity of the average doubly bridged Fe–I and Co–I bond lengths of 2.58 Å in $[Fe(NO)_2I]_2$ and 2.59 Å in $[Co(NO)_2I]_n$ indicates no noticeable effect on the totally different structures on these particular bond lengths. The iron radius of 1.25 Å and cobalt radius of 1.26 Å (obtained by subtraction of the above presumed single-bond covalent radii of the bridging atoms) are within the 1.24–1.32 Å range of iron radii derived from the Fe–N bond lengths in the iron tricarbonyl nitrogen dimers and are only slightly longer than the iron radii of range 1.22–1.23 Å derived from the Fe–SR bond lengths in $[Fe(NO)_2SC_2H_5]_2$ (Table VI, no. II), $[Fe(CO)_3SC_2H_5]_2$ (no. III), $[Fe(CO)_3SCC_6H_5]_2$, and $[Fe_2(CO)_6SCH_3]_2S$. In contrast, much shorter cobalt and nickel radii of 1.06 and 1.05 Å, respectively, are acquired from the doubly bridged $Co\text{–}P(C_6H_5)_2$ bond lengths of 2.16_0 Å in $[Co(\pi\text{-}C_5H_5)P(C_6H_5)_2]_2$ (no. V) and the $Ni\text{–}P(C_6H_5)_2$ bond length of 2.15 Å in $[Ni(\pi\text{-}C_5H_5)P(C_6H_5)_2]$ (no. XVII). The relative metal radii differences for these iodine and other ligand-bridged complexes support and extend the previously drawn interpretations (which were initially made from a direct comparison of M–B bond length measurements) that π-bonding character is considerable for bridging PR_2 groups, much less important for bridging SR groups, and still less important (and probably of little consequence) for bridging halogen atoms. As expected, the largest iron radii occur for the bridging NR_2 groups which do not have energetically favorable d orbitals available to form multiple bonds. This explanation of the observed over-all trend towards smaller M–B bond lengths (or smaller metal radii) with different bridging ligands as due primarily from an energetic viewpoint to the multiple-bonding capabilities of the bridging ligands (*i.e.*, for similar R groups, in general $PR_2 \gg SR > I > NR_2$) is valid only in the absence of pronounced steric effects but otherwise is neither unreasonable nor inconsistent with other experimental and theoretical evidence for the existence of d-orbital multiple bonding with these ligands.

magnetism) the long observed distance in the mercaptoiron dimer precludes the possibility of the iron–iron bond having any appreciable bond strength or any influence on the molecular geometry. In connection with a proposal of a strong "bent" iron–iron single bond being responsible for the molecular geometry in $[Fe(CO)_3SC_2H_5]_2$ with the remarkably acute Fe–S–Fe bridging angles of 68°, Dahl and Wei[46] postulated that despite its rather long Fe–Fe distance the sharply acute bridging angles of 74° in $[Fe(NO)_2SC_2H_5]_2$ may likewise be a consequence of the iron–iron bond which pulls the iron atoms as close together as possible. They also pointed out from a valence-bond representation based on a tetrahedral-like environment about each iron atom that the formation of a distinct iron–iron σ bond can occur in $[Fe(NO)_2SC_2H_5]_2$ by direct overlap of equivalent d_{z^2}–s–p_z hybrid iron orbitals compounded in some unknown degree from the atomic valence orbitals.

An equivalent but more general formulation of the nature of the Fe–Fe bond in any $[Fe(NO)_2X]_2$ complex ($X = SC_2H_5$, I, or other ligand containing a three-electron donor B atom) can be obtained from simple MO symmetry arguments. Local right-handed coordinate systems were chosen at each iron atom with the z axis directed along the iron–iron line, the x axis oriented in the plane of the Fe_2B_2 rhombus, and the y axis perpendicular to this plane. The nine valence atomic orbitals on each iron atom can be classified together by linear combination into 18 localized iron symmetry orbitals which transform according to the irreducible representations of the molecular point group D_{2h}. Of these the s, p_z, and d_{z^2} combinations are of σ symmetry relative to the iron–iron line, the p_x, p_y, d_{xz}, and d_{yz} combinations analogously have π symmetry, and the d_{xy} and $d_{x^2-y^2}$ combinations possess δ symmetry. The large distance between the iron atoms necessarily will result in small energy differences between the two formally bonding and antibonding combinations of the same AO's. The energy separation will be largest for the σ orbitals (*e.g.*, the $(1/\sqrt{2})(4d_{z^2} + 4d_{z^2}')$ and $(1/\sqrt{2})(4d_{z^2} - 4d_{z^2}'))$ which overlap to a greater extent than the corresponding π or δ orbitals. Eight of these iron symmetry orbitals are regarded under the perfect-pairing approximation to interact primarily with eight appropriate symmetry combinations of bridging B and nitrosyl nitrogen atoms to form eight bonding and eight antibonding localized iron–ligand σ-type MO's of which only the bonding MO's are occupied with two electrons each. For the above choice of local axes, this σ bonding was presumed from the approximate tetrahedral ligand environment about each iron atom to involve the eight s, p_x, p_y, and p_z symmetry orbital combinations; the arbitrary choice of these particular iron symmetry orbitals from the symmetry classifications allowed for the metal–ligand σ bonding has no qualitative effect on the results. After allowance of the eight electron pairs for this bonding, there remain 18 valence electrons to be allotted to the remaining 10 metal symmetry orbitals of which from overlap considerations the d_{z^2} bonding combination is of the lowest relative energy and its antibonding combination of the highest relative energy. The seemingly reasonable assumption made here is that the tetrahedral-like ligand field energy splittings of the σ, π, and δ d orbitals of each iron atom as a result of their interactions with the ligands are sufficiently small relative to the energy shift produced by the interaction of the d_{z^2} iron orbitals with each other so as not to displace the antibonding d_{z^2} level as the one of highest relative energy. The addition of the 18 electrons to these 10 metal symmetry orbitals thereby results in all energy levels being filled except the least stable antibonding d_{z^2} one. Since the superposition of the bonding and antibonding localized MO's when both are completely occupied with electrons leads to "no bonding" or to a small degree of antibonding, the net contribution to the iron–iron interaction is the formation of a direct electron-pair σ bond in accord with the closed-shell electronic configuration for each iron atom. The above treatment restricted this σ orbital to pure d_{z^2} character but just as well could have embraced a d_{z^2}–s–p_z hybrid combination. Hence, both the valence-bond and MO approaches lead to the same conclusion that a distinct, direct electron-pair σ bond can stabilize these iron nitrosyl dimers.

(c) Consequences of the Fe–Fe Bond. The metal-metal interaction in $[Fe(NO)_2I]_2$ as well as in $[Fe(NO)_2SC_2H_5]_2$ is proposed to have two significant stereochemical consequences. First, it accounts for the observed identical geometrical distortion of the Fe_2B_2 framework in each molecule with the sharply acute Fe–B–Fe bridging angles of 73–74° compared to the M_2B_2 framework with larger (and more normal) M–B–M′ angles that are found in molecules containing tetrahedrally coordinated metal atoms for which no metal–metal interactions occur. (In Table VI such molecules include no. VIII, X, XII, XIII, XIV, XVIII, and XIX for which the M–B–M′ angular range is 82–92°.) Secondly, it is rationalized that the different kind and degree of polymerization of $Fe(NO)_2I$ and $Co(NO)_2I$ in their respective solid-state structures must be attributed to the energy stabilization of the dimeric geometry for the iron complex by the formation of the electron-pair Fe–Fe bond. The driving force is the net bonding energy gained by the occupancy of only the bonding metal symmetry orbital combination (*i.e.*, the $(1/\sqrt{2})(4d_{z^2} + 4d_{z^2}')$ in the previous MO formulation) with two electrons. In the case of an analogous cobalt dimer, the two additional electrons would go into the corresponding antibonding metal symmetry orbital combination (*i.e.*, the $(1/\sqrt{2})(4d_{z^2} - 4d_{z^2}')$ orbital) which would result in a net energy destabilization with no direct bond between the cobalt atoms. From interelectronic repulsion considerations this nonbonding effect in turn would substantially increase the cobalt–cobalt distance and through a concomitant widening of the Co–I–Co angles of the Co_2I_2 rhombus would necessarily decrease the nonbonding I···I contact. The resulting equilibrium geometry apparently renders the iodine-bridged cobalt dimer unstable in the solid state relative to the infinite polymer found for $[Co(NO)_2I]_n$. The fact that cobalt dinitrosyl chloride forms a solid-state dimer[18-20] whereas the bromide complex possesses the infinite chain structure[18] indicates that the M–B bond length as determined primarily by the size of the bridging atom and/or the effective electronegativity of the bridging atoms plays a dominant role in the stabilization of the dimeric structure (*vide infra*).

(d) Mass Spectrometric Evidence for the Presence of an Iron–Iron Bond. Our view of the importance of the iron–iron interactions in the stabilization of the geometries of the iron nitrosyl halide and mercapto dimers is in

---

[46] L. F. Dahl and C. H. Wei, *Inorg. Chem.*, **2**, 328 (1963).

harmony with the mass spectrometic interpretations by Johnson, Lewis, Williams, and Wilson,[47] who recently showed that the fragmentation patterns of the iron nitrosyl halide complexes $[Fe(NO)_2X]_2$ (where X = Cl, Br) are similar to one another but markedly different from those of the cobalt nitrosyl halide complexes $[Co(NO)_2X]_2$ (where X = Cl, Br, I) which were all established as containing dimeric molecules in the gas phase.[48] These English workers[47] suggested that the significant difference between the primary fragmentation patterns of the iron and cobalt nitrosyl halides is related to the presence of the metal–metal interaction in the iron complexes which stabilizes the Fe_2X_2 rhombus relative to the loss of nitric oxide. The mass spectral patterns of $[Fe(NO)_2SR]_2$ and $[Co(NO)_2SR]_2$ were observed by Johnson, Lewis, and coworkers[47] to be more complex with the metal–sulfur rhombus system for both iron and cobalt being the most stable grouping in the molecule and with the decomposition patterns being more dependent on the nature of the side chain of the thiol than on the metal ion. Nevertheless, the different mass spectra of the phenylmercaptometal nitrosyl dimers of iron and cobalt were correlated[47] with the presence of the metal–metal interaction in the iron dimer.

Of prime significance is that our mass spectrum of $[Fe(NO)_2I]_2$ whose major peaks are given in Table V is similar to the mass spectra of the chloride and bromide iron analogs, and hence the mass spectrometric results are in complete accord with our interpretations of the X-ray results concerning the considerable strength of the iron–iron interactions in these dimeric iron nitrosyl complexes. Our mass spectrum of cobalt nitrosyl iodide is essentially the same as that reported by Johnson, Lewis, and coworkers.[47]

The Metal–Nitrosyl System. Another implication of the Fe–Fe bonding schemes applied to $[Fe(NO)_2SC_2H_5]_2$ and $[Fe(NO)_2I]_2$ is that to the extent the d_{z^2} orbital on each iron atom participates in the Fe–Fe bonding, it presumably is not available for the $d\pi$ bonding with the two nitrosyl ligands.[49,50] Hence, it is expected that greater π bonding between the metal and nitrosyl ligands should take place in the $[Co(NO)_2I]_n$ complex where with no metal–metal bond both the filled bonding and antibonding d_{z^2} cobalt combinations are essentially free for interaction with the π^* nitrosyl orbitals. Support for this theoretical prediction is indicated from the somewhat marginally significant shorter average Co–N bond length of 1.61 Å in $[Co(NO)_2I]_n$ compared to the average Fe–N bond lengths of 1.67 Å in both $[Fe(NO)_2I]_2$ and $[Fe(NO)_2SC_2H_5]_2$.

These short metal–nitrogen bond lengths, which are indicative of strong multiple bonding between the NO groups and the metal atoms, are also consistent with the mean Fe–NO bond distances in $Na_2Fe(CN)_5(NO)\cdot 2H_2O$ (1.63 ± 0.02 Å),[51] $CsFe_4S_3(NO)_7\cdot H_2O$ (1.67 Å; indiv esd, 0.04 Å for the six NO groups coordinate to the three equivalent basal iron atoms),[33] and $Fe(NO)[S_2CN(CH_3)_2]_2$ (1.63 ± 0.02 Å).[52] The NO bond lengths of 1.15 Å in $[Fe(NO)_2I]_2$ and 1.19 Å in $[Co(NO)_2I]_n$ also compare favorably with those in $[Fe(NO)_2SC_2H_5]_2$ (1.17 Å; indiv esd, 0.02 Å),[14] $Na_2Fe(CN)_5NO\cdot 2H_2O$ (1.13 ± 0.02 Å),[51] $CsFe_4S_3(NO)_7\cdot H_2O$ (1.20 Å; indiv esd, 0.06 Å),[33] and $Fe(NO)[S_2CN(CH_3)_2]_2$ (1.19 ± 0.03 Å).[52]

In contrast to the essentially linear Fe–N–O angle of 178.3° in sodium nitroprusside,[51] the nitrosyl groups are inclined with respect to the metal–nitrogen bond over an angular range of 157–165° in $[Fe(NO)_2I]_2$ and 168–172° in $[Co(NO)_2I]_n$. Similar nonlinear Fe–N–O linkages have been found in $[Fe(NO)_2SC_2H_5]_2$ (where the two angles are 167 and 168°),[14] $CsFe_4S_3(NO)_7\cdot H_2O$ (where deviations extend to 20°),[33] and $Fe(NO)[SC_2CN(CH_3)_2]_2$ (where the angle is 158°).[52] These bent Fe–N–O groupings can be rationalized as a combined effect of both crystal packing forces and electronic effects involving the different degrees of usage of the two nondegenerate π and two nondegenerate π^* orbitals on each NO in their bonding with the appropriate metal atom orbitals.

M_2B_2 Bridged Systems with and without Metal–Metal Interactions. (a) General Remarks. In an effort not only to provide supporting evidence for the hypothesis that the metal–metal bond is the controlling influence for the solid-state dimerization of $Fe(NO)_2I$ as opposed to the possible alternative polymeric structure of $[Co(NO)_2I]_n$ but also to assess the various factors which together energetically determine the stability of the $Fe(NO)_2I$ and $Co(NO)_2Cl$ complexes as dimers and the $Co(NO)_2Br$ and $Co(NO)_2I$ complexes as infinite chains, the structural features of a large number of ligand-bridged molecules containing four-membered M_2B_2 ring systems have been carefully examined. Table VI lists the pertinent molecular parameters of representative complexes which are categorized according to whether or not they contain metal–metal interactions. A further ranking of these complexes is made on the basis of the kind of bridging atoms. Unfortunately, reasonably accurate structural data exist for only a few compounds in which bromine and iodine are the bridging atoms.

These and other structural data now accumulated show that the particular coordination about each metal atom in ligand-bridged dimers plays a more influential role than previously suspected in dictating the kind of deformation of the M_2B_2 system resulting from a metal–metal interaction. Hence, the effects of the metal–metal interactions on the M_2B_2 systems are presented below on the basis of resulting metal coordination number which includes the metal-bonded atom.

(b) Five-Coordinated Metal Atoms. For an M_2B_2-bridged system containing a tetrahedral-like environment about each metal atom, the metal–metal interaction simply produces a planar deformation of the M_2B_2 system of the variety as found in $[Fe(NO)_2I]_2$ and $[Fe(NO)_2SC_2H_5]_2$ in order to decrease the metal–metal distance as much as possible. The observed dependence of the iron–iron

---

(47) B. F. G. Johnson, J. Lewis, I. G. Williams, and J. M. Wilson, *J. Chem. Soc., A*, 338 (1967); J. Lewis and B. F. G. Johnson, *Accounts Chem. Res.*, **1**, 245 (1968).

(48) During sublimation of cobalt nitrosyl iodide partial decomposition of the crystalline sample was observed to occur with noticeable liberation of pure iodine vapor. Furthermore, the mass spectrometric fragmentation patterns of the cobalt dinitrosyl halides do not exclude the possibility that the vapor phase may be comprised of monomeric paramagnetic species (such as $Co(NO)_2I_2$) as well as dimeric molecules.

(49) In regular tetrahedral XQ_4^{n-} ions (X = Si, P, S, or Cl) of T_d point group, the degenerate d_{z^2} and $d_{x^2-y^2}$ orbitals of representation E are found[50] from overlap considerations to form much stronger π-bonding MO's than the other three degenerate d orbitals which belong to the same representation (T_2) as the triply degenerate p orbitals.

(50) D. W. J. Cruickshank, *J. Chem. Soc.*, 5486 (1961).

(51) P. T. Manoharan and W. C. Hamilton, *Inorg. Chem.*, **2**, 1043 (1963).

(52) R. P. White, J. A. McCleverty, and L. F. Dahl, submitted for publication.

distances on the size of bridging atoms in these two iron complexes can be readily understood.

This unusual kind of five-coordination can also be invoked for $Al_2(CH_3)_6$ and B_2H_6 to the extent that a direct metal–metal interaction is deemed a significant part of the bonding of the bridged M_2B_2 system.[53–58] In connection with their recent X-ray refinement of the $Al_2(CH_3)_6$ structure, Vranka and Amma[59] reexamined the factors put forth by Rundle[60] to rationalize the stability of alkyl-bridged dimers. From additional data Vranka and Amma[59] concluded that two factors proposed by Rundle[60] were important in favoring dimeric association: *viz.* (1) a large bond energy for a normal single bond between the metal and carbon atom, and (2) a minimal amount of inner-shell repulsion between the two metal atoms separated by internuclear distances demanded by the geometry of the dimer. They also suggested that two additional factors, which conformed to the molecular parameters of $Al_2(CH_3)_6$, could not be neglected: *viz.* (1) steric repulsions including those between the terminal ligands and bridging ligands as well as between the two bridging ligands, and (2) direct metal–metal bonding.

From a systematic examination of molecular complexes containing M_2B_2 systems formed by group IIa and IIIa metal atoms (without metal–metal interactions), Magnuson and Stucky[61] recently showed for R_3C-, R_2N-, R_2CN-, RO-, Cl-, and Br-bridged species that the four-membered heterocyclic ring systems depend upon the kind of bridging atoms. Although they noted in many complexes the relative insensitivity of the M–B–M′ bridging angle to a change of metal atom and ligands external to the M_2B_2 ring, they also pointed out that steric repulsions from externally attached ligands can be important in complexes such as $[Be(CH_3)_2]_n$ and $[BeCl_2]_n$ where close contacts occur between atoms on adjacent rings. The more acute bridge angles in these polymeric beryllium complexes were explained as resulting from a minimization of the above-mentioned inter-ring nonbonded repulsions. The other major correlation made by Magnuson and Stucky[61] was that the smaller bridging angles found for the halogen-bridged dimeric molecules (with tetrahedrally coordinated metal atoms but containing no metal–metal interactions) appear to be due primarily to the halogen–halogen repulsions across the ring (except for a few cases such as $[BeCl_2]_n$ where inter-ring Cl$\cdots$Cl repulsions are also important). In this regard they also noted that in many complexes the halogen–halogen contact distances appeared to be fairly constant.

(c) Six-Coordinated Metal Atoms. A number of diamagnetic iron carbonyl complexes of general type $[Fe(CO)_3X]_2$ (where X represents a bridging three-electron donor such as NR_2, PR_2, SR, or one-half of a bidentate group such as RNCONR′, RNC_6H_4NR', or $R_2C_2S_2$) containing strong iron–iron bonds have been structurally characterized by X-ray diffraction studies.[36,38,46,62–72] The basic dimeric framework of the $[Fe(CO)_3X]_2$ molecule formally arises from the intersection of two distorted $Fe(CO)_3X_2$ tetragonal pyramids along the common basal X_2 edge. A detailed structural comparison[36] shows that despite sterically predictable variations in the B–Fe–B angles of the Fe_2B_2 system (B = N, P, S) in these homologous complexes, there is an over-all uniformity of the bonding Fe–Fe distances and Fe–B–Fe angles for a given B bridging atom. The considerably shorter Fe–Fe distances in the nitrogen-bridged dimers (2.37–2.40 Å) compared to the sulfur-bridged dimers (2.51–2.55 Å) are found to be primarily an outcome of the much smaller Fe–B distances (1.94–2.02 Å *vs.* 2.23–2.27 Å) counterbalanced to some extent by the somewhat larger Fe–B–Fe angles (72–75° *vs.* 67–70°).[36] Table VI lists as representative examples the pertinent molecular parameters of $[Fe(CO)_3SC_2H_5]_2$ (no. III) and $[Fe(CO)_3NH_2]_2$ (no. IV). Two electronically equivalent $[Co(\pi\text{-}C_5H_5)X]_2$ complexes (where the π-C_5H_5 group can be stereochemically considered to occupy three coordination sites) with X equal to $(C_6H_5)_3P$ and $(t\text{-BuN})_2CO$ have been shown from X-ray investigations[70–72] to be structurally related to their iron tricarbonyl counterparts. The close resemblance of the molecular configurations of $[Co(\pi\text{-}C_5H_5)P(C_6H_5)_2]_2$ (no. V),[70] $[Fe(CO)_3SC_2H_5]_2$ (no. III),[46] and $[Fe(CO)_3NH_2]_2$ (no. IV)[36] is readily seen from a comparison of the corresponding angular parameters (given in Table VII) which show a near-unalterability of the M_2B_2 framework on exchange of a stereochemically functioning tridentate π-$C_5H_5^-$ ring in place of three unidentate carbonyl groups.

In all of these sulfur-, nitrogen-, and phosphorus-bridged complexes, the short metal–metal distances arising from electron-pair bond formation are achieved by a bending deformation of the M_2B_2 framework along the B$\cdots$B line from a planar M_2B_2 system of dihedral angle

---

[53] For a pertinent discussion of recent theory and experimental data relevant to bonding in B_2H_6, see E. L. Muetterties and W. H. Knoth, "Polyhedral Boranes," Marcel Dekker, Inc., New York, N. Y., 1968, pp 32–37.

[54] Of the three most rigorous molecular orbital bonding treatments[55–57] of diborane which indicate that the gross atomic charge separations have been seriously overestimated in all other approximate treatments,[58] the ones[55,56] with Gaussian basis functions show that the ground-state electron density distribution of the B_2H_2 rhombus of diborane is mainly concentrated in two three-center electron-pair bonds involving practically no bond between the boron atoms. In contrast, the rigorous molecular SCF-LCAO calculations[57] which utilized a nearly optimized minimal set of Slater-type orbitals yielded a moderately strong direct B–B interaction in agreement with all other more approximate calculations.

[55] L. Burnelle and J. J. Kaufmann, *J. Chem. Phys.*, **43**, 3540 (1965), and references cited therein.

[56] R. J. Buanker, S. D. Payerimhoff, L. C. Allen, and J. L. Whitten, *ibid.*, **45**, 2835 (1966).

[57] W. E. Palke and W. N. Lipscomb, *J. Am. Chem. Soc.*, **88**, 2384 (1966), and references cited therein.

[58] For recent approximate calculations with references to earlier calculations, see (a) B. J. Duke and J. W. Linnett, *Trans. Faraday Soc.*, **62**, 2955 (1966); (b) T. Ogawa and K. Hirota, *J. Mol. Spectry.*, **21**, 29 (1966).

[59] R. G. Vranka and E. L. Amma, *J. Am. Chem. Soc.*, **89**, 3121 (1967).

[60] R. E. Rundle, *J. Phys. Chem.*, 61, 45 (1957); P. H. Lewis and R. E. Rundle, *J. Chem. Phys.*, **21**, 986 (1953).

[61] V. R. Magnuson and G. D. Stucky, *J. Am. Chem. Soc.*, **90**, 3269 (1968); G. D. Stucky, private communication to L. F. Dahl, 1968.

[62] H. P. Weber and R. F. Bryant, *J. Chem. Soc.*, 182 (1967).

[63] J. M. Coleman, A. Wojcicki, P. J. Pollick, and L. F. Dahl, *Inorg. Chem.*, 6, 1236 (1967).

[64] C. H. Wei and L. F. Dahl, *ibid.*, 4, 1 (1965).

[65] P. E. Baikie and O. S. Mills, *Chem. Commun.*, 707 (1966); P. E. Baikie and O. S. Mills, *Inorg. Chim. Acta*, **1**, 55 (1967).

[66] M. M. Bagga, P. E. Baikie, O. S. Mills, and P. L. Pauson, *Chem. Commun.*, 1106 (1967).

[67] J. A. J. Jarvis, B. E. Job, B. T. Kilbourn, R. H. B. Mais, P. G. Owston, and P. F. Todd, *ibid.*, 1149 (1967).

[68] D. Bright and O. S. Mills, *ibid.*, 245 (1967).

[69] J. Piron, P. Piret, and M. Van Meerssche, *Bull. Soc. Chim. Belges*, 76, 505 (1967).

[70] J. M. Coleman and L. F. Dahl, *J. Am. Chem. Soc.*, **89**, 542 (1967).

[71] Y. Matsu-ura, N. Yasuoka, T. Ueki, N. Kasai, M. Kakudo, T. Yoshida, and S. Otsuka, *Chem. Commun.*, 1122 (1967).

[72] S. Otsuka, A. Nakamura, and T. Yoshida, *Inorg. Chem.*, **7**, 261 (1968).

180° to a nonplanar M_2B_2 system containing sharply acute M–B–M angles. The resulting six-coordination about each metal atom can be conceptually viewed as octahedral-like with a "bent" metal–metal bond occupying the sixth coordination site about each metal atom. The considerable degree of influence of a metal–metal bond on this kind of molecular geometry was first illustrated[70] by the drastic alteration of the M_2B_2 skeleton in the diamagnetic dimers $[Co(\pi\text{-}C_5H_5)X]_2$ and $[Ni(\pi\text{-}C_5H_5)X]_2$ ($X = P(C_6H_5)_2$) (Table VI, no. V and XVII, respectively) for which the genesis of a "bent" cobalt–cobalt electron-pair bond in the former complex has decreased the cobalt–cobalt distance from a nonbonding value of 3.36 Å in $[Ni(\pi\text{-}C_5H_5)P(C_6H_5)_2]_2$ to a bonding value of 2,56 Å in $[Co(\pi\text{-}C_5H_5)P(C_6H_5)_2]_2$. This remarkable decrease of 0.70 Å in the metal–metal distance is a consequence of a bending of the M_2P_2 rhombus along the P···P line from a 180° dihedral angle in the planar Ni_2P_2 rhombus to a dihedral angle of 105° in the bent Co_2P_2 system; the degree of angular distortion results in a decrease of the bridging M–P–M′ angle by 30° from a normal unstrained Ni–P–Ni′ value of 102° in the nickel complex to the sharply acute Co–P–Co′ angle of 72.5° in the cobalt analog.

(d) Seven-Coordinated Metal Atoms. The diamagnetic complex α-$[NbI_4]_n$ (no. VI)[73] exemplifies the case of a planar deformation of a M_2B_2 rhombus in normally octahedrally coordinated metal complexes due to a metal–metal interaction. An electron-pair coupling between pairs of niobium(IV), each of which normally contains one unpaired electron, results in a considerable distortion of the infinite chain geometry of NbI_6 octahedra fused together at opposite edges.[73] Formation of direct Nb–Nb bonds (which thereby increases the coordination number of each niobium to seven) results in a planar deformation of the Nb_2I_2 systems containing the Nb–Nb bonds such that the internuclear Nb–Nb separations are decreased to 3.31 Å and the bridging Nb–I–Nb angles are only 74° in contrast to the nonbonding distances of 4.36 Å and the obtuse bridging Nb–I–Nb angles of 98° in the adjacent Nb_2I_2 rhombi which contain no Nb–Nb bonds. Similarly, in the solid $[NbI_5]_2$ (no. IX)[74] where no bonding electronic effects determine the stereochemistry of the dimeric units (each of which is comprised of two NbI_6 octahedra joined at a common edge), the average Nb–I–Nb bridging angle is 100° and the nonbonding Nb–Nb distance is 4.55 Å. The bonding Nb–Nb distances of 3.31 Å in α-$[NbI_4]_n$ are the longest known values observed in any polynuclear niobium complex containing Nb–Nb interactions.[75–77] It is obvious that steric compression effects of the bridging iodine atoms prevent closer Nb–Nb bonding distances which in turn would give even more acute Nb–I–Nb′ bridging angles and therefore greater interorbital bonding electron-pair repulsions on the bridging iodine atoms. These conclusions are in accord with the observed longer Nb–Nb distances for other seven-coordinated niobium complexes containing Nb_2B_2 rhombi relative to the considerably shorter ones found in niobium metal (2.86 Å) and in the niobium halide cluster systems of $[Nb_6X_{12}]^n$ and $[Nb_6X_8]^n$.[75–77] Furthermore, the Nb–Nb bonding distances in Nb_2B_2 rhombi of structurally analogous complexes can be correlated with the size (and effective electronegativity) of the bridging B atoms. For example, the Nb–Nb bonding distance of 3.06 Å in $NbCl_4$, which is isomorphous with α-$[NbI_4]$, is 0.25 Å less than that in α-$[NbI_4]$ as expected for smaller, electronegative bridging halogen atoms. In such complexes possessing bonding pairs of seven-coordinated metal atoms, it again must be emphasized that nonbonding repulsions involving the other ligands may also strongly influence the metal–metal distance.

A similar planar distortion of an M_2B_2 rhombus by an electronic interaction to give seven-coordinated metal atoms occurs in both the solid-state molybdenum dimers $[Mo(OC_6H_5)_3Cl_2]_2$[78] and $[Mo(CO)_4P(CH_3)_2]_2$,[79] where two octahedra are joined at a common edge by two chlorine bridges in the former molecule and by two phosphido bridges in the latter molecule. In contrast to the nonbonding distance of 3.84 Å in the structurally similar $[MoCl_5]_2$ dimer[80] (which has a normal magnetic moment corresponding to one unpaired electron per Mo(V)), the relatively short Mo–Mo bonding distance of 2.8 Å and low observed magnetic moment in the phenoxide analog,[78] and the Mo–Mo bond value of 3.09 Å and the observed diamagnetism in the carbonyl complex,[79] are prime evidence for Mo–Mo bonds. The considerable strength of the metal–metal bond in each of these two ligand-bridged dimers should be reflected not only in the bonding Mo–Mo distance but also in its pronounced steric effect on the M_2B_2 rhombus as given by the Mo–B–Mo bridging angles. Although no structural details are yet available for $[Mo(OC_6H_5)_3Cl_2]_2$,[78] a normally occurring obtuse Mo–Cl–Mo bridging angle of 99° is found in $[MoCl_5]_2$ whereas the Mo–P–Mo angle in $[Mo(CO)_4P(CH_3)_2]_2$ is only 78°.

Other typical octahedrally coordinated metal dimers possessing planar M_2B_2 ring systems without metal–metal interactions are $[NbCl_5]_2$ (no. XVI),[81] $[ReCl_5]_2$,[82] and $[Mn(CO)_4Br]_2$ (no. XX).[83] Their molecular parameters illustrate that the B–M–B angles generally are considerably less than 90° (and the M–B–M angles greater than 90°). The structures of $[NbCl_5]_2$, $[MoCl_5]_2$, and $[ReCl_5]_2$ are closely related to one another in that the nonbonding Cl···Cl distances outlining the dimeric octahedra are all rather constant values ranging from 3.2 Å from the centers of the chlorine octahedra along the metal–metal line directions away from each other thereby resulting in the acute B–M–B angles of 79–81° range and obtuse M–B–M angles of 99–101° range. Mucker, *et al.*,[82] rationalized that these displacements of similar magnitude for the three chlorine-bridged dimers suggest a strong coulombic repulsion between the metal atoms (*i.e.*, the Nb···Nb distance is 3.95 Å, the Mo···Mo distance is 3.84 Å, and the Re···Re distance is 3.74 Å). On the other hand, the acute B–M–B bond angle at each niobium

---

(73) L. F. Dahl and D. L. Wampler, *Acta Cryst.*, **15**, 903 (1962).

(74) L. F. Dahl and N. Nelson, unpublished research.

(75) For an extensive tabulation of metal–metal distances for polymeric transition metal halide and oxide complexes, see H. Schafer and H. G. Schnering, *Angew. Chem.*, 76, 833 (1964).

(76) H. G. Schnering and W. Beckmann, *Z. Anorg. Allgem. Chem.*, **347**, 231 (1966), and references cited therein.

(77) L. R. Bateman, J. F. Blount, and L. F. Dahl, *J. Am. Chem. Soc.*, **88**, 1082 (1966), and references cited therein.

(78) Mitchell and Prout, unpublished work; *cf.*, P. C. H. Mitchell and R. J. P. Williams, *J. Chem. Soc.*, 4570 (1962).

(79) R. H. B. Mais, P. G. Owston, and D. T. Thompson, *ibid.*, *A*, 1735 (1967).

(80) D. E. Sands and A. Zalkin, *Acta Cryst.*, **12**, 723 (1959).

(81) A. Zalkin and D. E. Sands, *ibid.*, **11**, 615 (1958).

(82) K. Mucker, G. S. Smith, and Q. Johnson, *ibid.*, **B24**, 874 (1968).

(83) L. F. Dahl and C. H. Wei, *ibid.*, 16, 611 (1963).

in $[NbCl_5]_2$ has been attributed by Gillespie[84] to bonding electron-pair repulsions which distort the octahedral arrangement of chlorine atoms around each niobium. This particular angular deformation is qualitatively rationalized[84] in terms of a higher effective electronegativity for the bridging chlorine atoms than that for the terminal ones which thereby results in the electron pairs of the Nb–Cl (bridging) σ bonds occupying less of the surface of the niobium atom than the other electron pairs of the Nb–Cl (terminal) σ bonds.

Hypothetic Solid-State $[Co(NO)_2I]_2$ Dimer *vs.* Observed Solid-State $[Co(NO)_2I]_n$ Chain. The fact that $Co(NO)_2I$ prefers a chain structure rather than a dimeric one whereas $Co(NO)_2Cl$ exists as a dimer in the solid state indicates that both the "effective" electronegativity and size of the bridging atom must be considered as factors which can influence the kind of structure present in the solid state. In the "ordered" dimer of $[Co(NO)_2Cl]_2$ the Co–Cl bonds are reported[20] as 2.13 and 2.33 Å (indiv esd, 0.03 Å); the reason for this distortion of the Co_2Cl_2 geometry from that of a rhombus is not apparent. The accuracy of these results[20] cannot be high owing to the incomplete refinement (*i.e.*, the final unweighted discrepancy *R* value was 15.6%) due to the twinning and/or disorder apparently involving only the other atoms in the unit cell. Nevertheless, the nonbonding intra-ring Cl···Cl distance of 3.12 Å is within the observed range of values found in other chlorine-bridged dimers (see Table VI); the reported Co···Co distance is 3.20 Å, and the Co–Cl–Co angle is 92°.[20]

With the assumption that $Co(NO)_2I$ as a dimer would possess a Co_2I_2 geometry of D_{2h} symmetry with a Co–I bond length of 2.59 Å and a nonbonding I···I distance of 3.86 Å (*i.e.*, these distances are found in $[Co(NO)_2I]_n$), the calculated Co···Co distance is 3.46 Å, the Co–I–Co angle 84°, and the I–Co–I angle 96°. Even though the Co–Co distance for this assumed geometry is 0.26 Å longer than that observed in $[Co(NO)_2Cl]_2$, the nonbonding interelectronic repulsions between the cobalt atoms may still be stronger (due to the electronegativity difference of Cl and I) in the I-bridged complex than those in the Cl-bridged dimer.[85] It is noteworthy that the average nonbonding Nb···Nb distance of 4.55 Å in $[NbI_5]_2$ (no. IX) is 0.65 Å greater than that of 3.90 Å in $[NbCl_5]_2$ (no. XVI). Since the observed Co···Co nonbonding distance of 3.86 Å in $[Co(NO)_2I]_n$ (no. VII) is 0.40 Å larger than that in the hypothetical dimer, the cobalt–cobalt nonbonding coulombic repulsions in the chain structure must be considerably less than in the dimer structure. Also, the interorbital electron-pair repulsions would presumably be greater for the acute Co–I–Co angle of 84° in the assumed dimeric geometry than for the obtuse 96° angle found in $[Co(NO)_2I]_n$. It is obvious that if the Co···Co distance in the hypothetical dimer is larger, then the I···I contact would be smaller and the Co–I–Co angle larger. If crystal packing forces are not considered to be a main factor, these comparisons indicate that association to give a M_2B_2-bridged system in transition metal complexes would be stabilized by electronic interactions but would be destabilized by strong metal–metal repulsions which depend on both the size and effective electronegativity of the bridging atoms. The stability is governed not only by the minimization of all nonbonded repulsions between atoms but also by interorbital electron-pair interactions which for a more electronegative bridging atom favor a wider bridging angle.

Acknowledgments. This work was accomplished through the generous financial support of the National Science Foundation (GP-4919 at the University of Wisconsin and GP-5752 at the University of Arizona). E. R. de G. gratefully acknowledges the predoctoral fellowship granted by both the Consejo de Desarrollo Cientifico and Escuela de Quimica of the Universidad Central de Venezuela. The use of the CDC 1604 and 3600 computers at the University of Wisconsin Computing Center was made available through partial support of NSF and WARF through the University Research Committee. We are indebted to Professor Richard F. Fenske at the University of Wisconsin for helpful discussions.

---

(84) R. J. Gillespie, *Angew. Chem. Intern. Ed. Engl.*, 6, 819 (1967).

(85) Because of the higher "effective" electronegativity of chlorine than iodine, the bridging iodine atoms will be better σ donors than the chlorine atoms. The negative charge density at each cobalt atom should then be greater in the iodine complex, thereby causing a larger expansion of the filled cobalt orbitals. This effect in turn leads to a stronger nonbonding coulombic repulsion between the cobalt atoms at a given Co–Co internuclear separation in $[Co(NO)_2I]_2$ than that in $[Co(NO)_2Cl]_2$. In the case of the corresponding iron dimers, an increase in orbital size effect allows an equilibration of the Fe–Fe σ-bonding interaction (due mainly to maximization of orbital overlap) at a greater internuclear Fe–Fe distance. Hence, the different Fe–Fe bond lengths in these ligand-bridged dimers are not indicative of bond strength.